Preparation of $LiMn_2O_4$ Powders via Spray Pyrolysis and Fluidized Bed Hybrid System

Izumi Taniguchi, Keigo Matsuda, Hiroki Furubayashi, and Shinya Nakajima
Dept. of Chemical Engineering, Graduate School of Science and Engineering, Tokyo Institute of Technology, 2–12-1 Ookayama, Meguro-ku, Tokyo 152-8552, Japan

DOI 10.1002/aic.10841
Published online April 13, 2006 in Wiley InterScience (www.interscience.wiley.com).

A novel technique has been developed to directly produce fine ceramic powders from liquid solution using a spray pyrolysis and fluidized bed hybrid system. Using this technique, the preparation of lithium manganese oxides $LiMn_2O_4$, which are the most promising cathode materials for lithium-ion batteries, has been carried out for various superficial gas velocities U_0 = 0.30-0.91 m/s, static bed heights L_s = 50-150 mm, and medium particle sizes $d_{pm,g}$ = 294-498 μm. The resulting powders had spherical nanostructured particles that comprised primary particles with a few tens of nanometer in size, and they exhibited a pure cubic spinel structure without any impurities in the XRD patterns. Moreover, the as-prepared powders showed better crystallinity and smaller specific surface area than those by conventional spray pyrolysis. The effects of process parameters on powder properties, such as specific surface area and crystallinity, were investigated for a wide range of superficial gas velocities and static bed heights. An as-prepared sample was used as cathode active materials for lithium-ion batteries and the cell performance has been investigated. Test experiments in the electrochemical cell Li/1M $LiClO_4$ in PC/$LiMn_2O_4$ demonstrated that the sample prepared by the present technique was superior to that by the conventional spray pyrolysis and solid-state reaction method. *AIChE J,* 52: 2413–2421, 2006
Keywords: particle technology, electronic materials, fluidized bed reactor, spray pyrolysis, lithium-ion batteries

Introduction

The fluidized bed reactor has a unique capability of continuous powder handling, good mixing, a larger gas-solid contact area, and very high rates of heat and mass transfer. Thus, it has been widely applied in the field of chemical engineering. Its applications range from physical operations, like drying[1] and agglomeration[2] of particles, to chemical reactors for chemical coating,[3-6] coal pyrolysis,[7] and the removal of acid gases.[8,9]

Recently, Matsuda et al.[10] have also applied the fluidized bed reactor to the preparation of lithium manganese oxide $LiMn_2O_4$, which is the most promising cathode material for lithium-ion batteries, by drip pyrolysis and succeeded in the continuous synthesis of powder by this technique. However, the as-prepared powder has various morphologies and a wide particle size distribution. Huang et al.[11], Matsuda and Taniguchi,[12,13] and Taniguchi et al.[14] have already reported that the electrochemical properties of lithium manganese oxide are strongly affected by the particle properties, such as morphology, interior structure, specific surface area and crystallites, of $LiMn_2O_4$ particles.

Thus far, many soft chemistry methods, such as sol-gel,[15,16] coprecipitation,[17,18] citric acid,[19-21] and hydrothermal processes,[22] have been developed to synthesize $LiMn_2O_4$ powders with improved physical and chemical characteristics. Most solution-precipitated powders must undergo subsequent calci-

Correspondence concerning this article should be addressed to I. Taniguchi at itaniguc@chemeng.titech.ac.jp.

nation and milling steps, which are processes that can negate some of the advantages of the solution process. As a result, agglomerated powders with irregular shapes are obtained. In contrast, hydrothermally prepared powders can be directly produced in their required physical and chemical forms. However, the high-pressure requirements and the general difficulty in producing a wide range of multicomponent compositions often deter the consideration of hydrothermal techniques for the synthesis of ceramic powders.

Spray pyrolysis is well known as a continuous single-step process for the preparation of fine ceramic powders. Compared with those of particles prepared by soft chemistry methods, the particle size distribution is narrow and controllable from micrometer to submicrometer, the purity of the products is high, and the composition of the powders is easy to control. Moreover, nonagglomerated powders are obtained. Taniguchi et al.[23] have reported that spherical nanostructured $LiMn_2O_4$ and $LiM_{1/6}Mn_{11/6}O_4$ (M = Al, Ni, and Co) particles with a narrow size distribution could be prepared by the ultrasonic spray pyrolysis method.

In this study, we have developed a novel technique for directly producing fine ceramic powders from a liquid solution using a spray pyrolysis and fluidized bed hybrid system and synthesized spinel $LiMn_2O_4$ powders by this technique. The physical properties of powders, such as crystallite size, specific surface area, morphology, particle size, and interior structure, have been examined by X-ray diffraction (XRD) analysis, the Brunauer-Emmett-Teller (BET) method, field emission scanning electron microscopy (FE-SEM), and transmission electron microscopy (TEM), respectively. The as-prepared powders have been used as cathode active materials for lithium-ion batteries, and electrochemical studies have been carried out on the charge/discharge characteristics of the half cells at a current density of 0.2 mA/cm^2.

Experimental Section

Principle of fine ceramic powder synthesis

Figure 1 shows a scheme of the synthesis of fine ceramic powders using the spray pyrolysis and fluidized bed hybrid system. The precursor solution, which contains some metal salts, is atomized to droplets with more than 10 micrometers in size using a two-fluid atomizer or an ultrasonic atomizer. The generated droplets are carried to the top of the fluidized bed reactor by air and supplied into the inner tube of the reactor. When the droplets reach the bed, the droplet-to-solid particle conversion quickly progresses through the evaporation of solvent from droplets, precipitation, drying, and thermal decomposition of salt in the reactor, as illustrated in Step 1 of Figure 1. As a result, spherical solid particles with several micrometers in size are obtained in the bed, and are fluidized with coarse particles. Fine particles adhere to the surface of the coarse particles and are then fluidized with coarse particles in the bed. Thus, fine particles have a very long residence time in the bed,[24] and the sintering of fine particles progresses during this process, as illustrated in Step 2 of Figure 1. Finally, the fine particles are detached from the coarse particles by the collision between the fluidizing coarse particles. Then they are entrained from the reactor due to the difference in terminal velocity between the fine particles and the coarse particles, as illustrated in Step 3 of Figure 1. The resulting particles can be captured by using a cyclone and a bag filter. This is the principle of fine ceramic powder preparation using the spray pyrolysis and fluidized bed hybrid system.

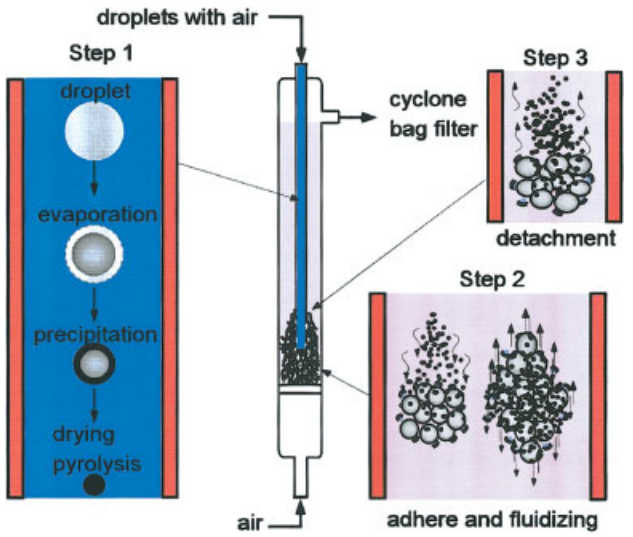

Figure 1. A scheme of the synthesis of fine ceramics powders via the spray pyrolysis and fluidized bed hybrid system.

[Color figure can be viewed in the online issue, which is available at www.interscience.wiley.com.]

Experimental apparatus and procedure

The experimental apparatus is shown in Figure 2. The apparatus consists of several major systems: a gas-flow control and measurement system, an atomization of precursor solution system, a fluidized bed reactor heated by electric furnaces (10), and a particle collection system. The droplet generation system consists of a two-fluid atomizer (7), a peristaltic pump (8) for supplying a precursor solution to the atomizer, and an air compressor (1) for supplying air to the atomizer. The fluidized bed reactor (11) is a cylindrical quartz tube of 61.5 mm in I.D. and 930 mm in effective length. A perforated plate with 2.4 percent open area (359 holes of 0.5 mm I.D. in 3 mm pitch) was used as a gas distributor. To supply the droplets in the fluidized bed reactor, a cylindrical quartz tube of 19.5 mm in I.D. and 1120 mm in length is inserted in the coaxial direction of the reactor. Structural details of the fluidized bed reactor are shown in Figure 3. Three external electronic furnaces (10) operated using PID controllers heated the reactor to 1073 K. To fluidize the coarse particles in the reactor, air was supplied to the bottom of the fluidized bed reactor by the compressor (2) through a packed column with 3-mm-diameter glass beads (3) and an orifice flowmeter. Spherical alumina particles were used as coarse fluidized medium particles. Their properties are summarized in Table 1. Before the preparation of $LiMn_2O_4$ powders using the spray pyrolysis and fluidized bed hybrid system, the surfaces of the alumina particles were coated with $LiMn_2O_4$ by drip pyrolysis in a fluidized bed reactor.[10]

The minimum fluidizing gas velocity U_{fm} was calculated

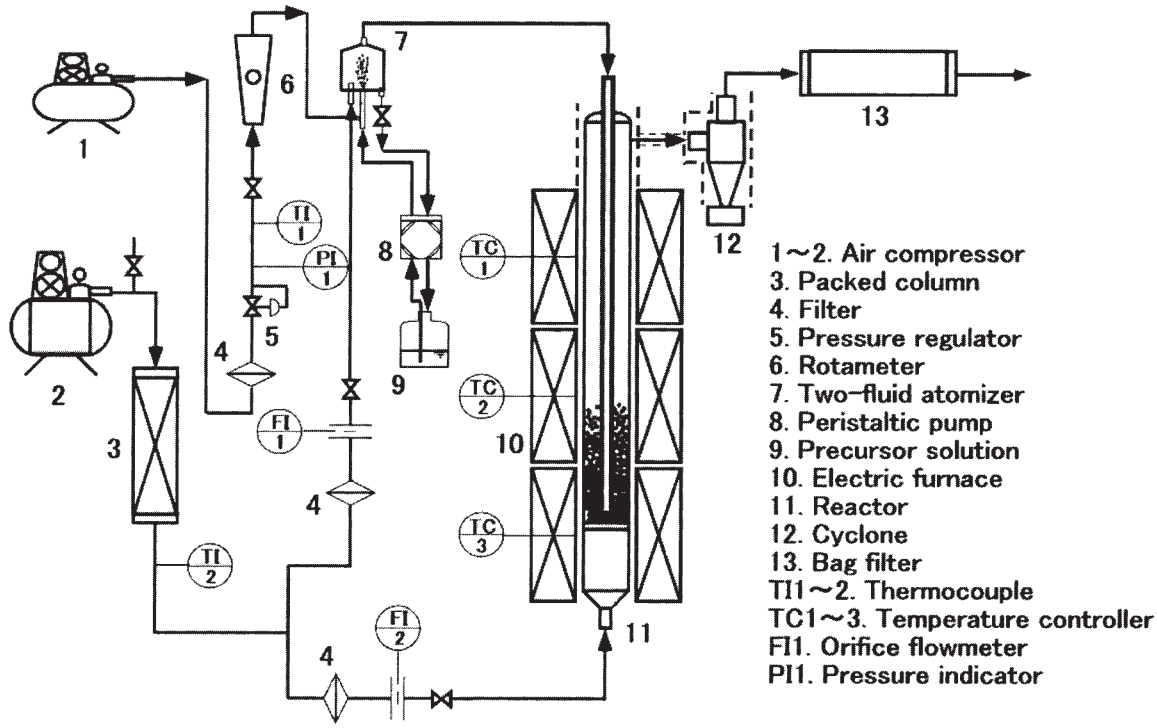

Figure 2. Experimental apparatus used for the spray pyrolysis and fluidized bed hybrid system.

using the correlation of Wen and Yu[25] after considering the effects of temperature on density and viscosity of gas.

The precursor solution was atomized using the two-fluid atomizer. The generated droplets were transported to the inner tube of the fluidized bed reactor by air. As described in the previous section, the droplet-to-solid particle conversion and sintering progress in the reactor. Finally, the fine particles are entrained from the reactor due to the difference in terminal velocity between the fine particles and the medium particles, and then the fine particles elutriated are collected using a cyclone (12) and a bag filter (13).

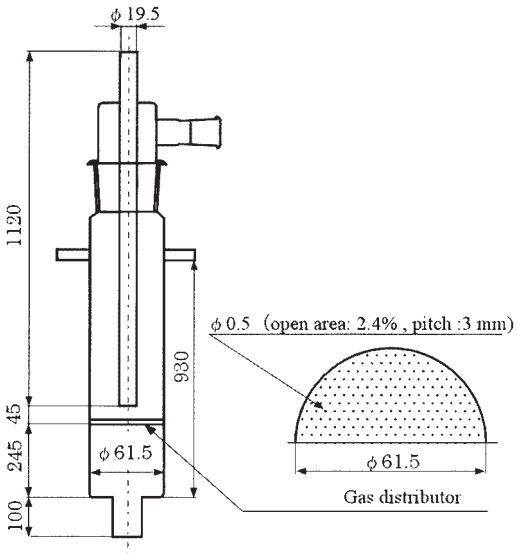

Figure 3. Details of fluidized bed reactor.

The precursor solution was prepared by dissolving a stoichiometric ratio of $LiNO_3$(98%) and $Mn(NO_3)_2$ $6H_2O$(98%) in distilled water. For all experiments, the total concentration C_0 was 3.0 mol/dm^3 and the atomic ratio of Li/Mn was set at 0.5. All chemicals were purchased from Wako Pure Chemical Industries Ltd., Tokyo, Japan.

The preparation of $LiMn_2O_4$ using the spray pyrolysis and fluidized bed hybrid system has been carried out at various U_0 = 0.30-0.91 m/s and static bed heights L_s = 50-150 mm.

Material characterization

The crystalline phase of the samples was also examined by X-ray diffraction analysis (XRD, Phillips, PW1700) at scan speeds of 2.4°/min for crystal analysis ranging from 4° to 70° and 0.6°/min for crystallite size measurements ranging from 40° to 50°. The crystallite size d was estimated from the (400) plane peak of XRD spectrum using Scherer's equation:

$$d = \frac{0.9\lambda}{(H - h)\cos\theta}, \tag{1}$$

Table 1. Properties of Fluidized Medium Particles

Particles	$d_{pm,g}$ [μm]	σ_g [·]	ρ_p [kg/m^3]	U_{mf} at 293 K [m/s]	U_{mf} at 1073 K [m/s]
Al_2O_3	294	1.31	3770	0.11	0.05
	478	1.11	3600	0.24	0.11

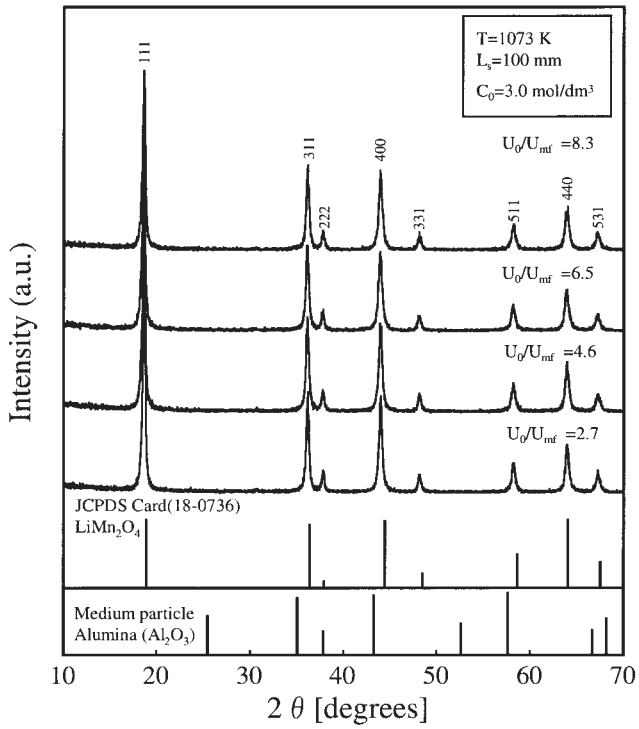

Figure 4. XRD patterns of $LiMn_2O_4$ powders synthesized at L_s = 100 mm and $d_{pm,g}$ = 498 μm for the range U_0/U_{mf} = 2.7-8.3.

where λ is the average of Cu Kα1 and Kα2; H, the full width at half maximum; h, the correction constant; and θ, the diffraction angle. Particle morphology was examined by field-emission scanning electron microscopy (FE-SEM, Hitachi, S-800) operated at 15 kV. The particle size distribution was determined by randomly sampling 500 particles from the SEM photographs. The geometric mean diameter $d_{p,g}$ and geometric standard deviation σ_g were calculated using

$$\ln d_{p,g} = \sum_{i=1}^{N} \frac{\ln d_{pi}}{N}, \tag{2}$$

$$\ln \sigma_g = \left[\frac{\sum_{i=1}^{N} (\ln d_{pi} - \ln d_{p,g})^2}{(N-1)} \right]^{1/2}, \tag{3}$$

respectively, in which N is the total number of samples. The interior structure of the as-prepared particles was observed by transmission electron microscopy (TEM, JEOL Ltd., JEM-200CX). The specific surface area of the as-prepared powders was measured by the Brunauer-Emment-Teller method (BET, FlowSorb II 2300, Shiraz Co.). The chemical composition of the as-prepared powders was determined by inductively coupled plasma-atomic emission spectroscopy (ICP-AES, Seiko Instruments Inc., SPS1500VR).

Fabrication and electrochemical characterization

A cathode electrode was prepared by mixing 75 wt% $LiMn_2O_4$ powders, 20 wt% acetylene black, and 5 wt% polytetrafluoroethylene (PTFE), and then formed into a thin film. A disk was cut off from the thin film and used as the cathode (5.4 mm diameter). The typical weight of the cathode was 2-3 mg. A lithium rechargeable cell consists of the cathode, an Li foil as the anode, a cellgard microporous membrane as the separator, and 1 mol/dm^3 $LiClO_4$ dissolved in propylene carbonate (PC) (<20 ppm H_2O, Tomiyama Pure Chemical Co., Ltd.) as the electrolyte.

Cell performance was evaluated using a potentiostat (HJR-110mSM6, Hokuto Denko) at a current density of 0.2 mA/cm^2 at room temperature. The cutoff voltage of the cycle was between 4.4 and 3.5 V. All charge/discharge measurements were carried out inside an argon-filled glove box. The procedures for the fabrication and the electrochemical measurements of lithium rechargeable cells Li/1M $LiClO_4$ in PC/$LiMn_2O_4$ are almost the same as those described previously.[14]

Results and Discussion

Sample characterization and powder properties

Figure 4 shows the X-ray diffraction patterns of the $LiMn_2O_4$ powders synthesized at L_s = 100 mm for the range U_0/U_{mf} = 2.7-8.3 using the spray pyrolysis and fluidized bed hybrid system. For the comparison between the XRD spectra of as-prepared powders and alumina, those of alumina (JCPDS 01–1243) are also shown in the figure. The diffraction peaks of all the samples corresponded to a single phase of cubic spinel structure with the space group $Fd\bar{3}m$ in which lithium ions occupy tetrahedral (8a) sites and manganese ions occupy octahedral (16d) sites. This suggests that there is no contamination of alumina in the resulting powders. The observed chemical compositions are shown in Table 2. The results were in good agreement with the one of the precursor solution (Mn/Li = 2). The same results were also obtained for the range L_s = 50-150 mm.

Figure 5 shows an example of SEM and TEM photographs of the $LiMn_2O_4$ powders synthesized at L_s = 100 mm and U_0/U_{mf} = 6.5 using the spray pyrolysis and fluidized bed hybrid system. It is clearly observed from the figure that the as-prepared $LiMn_2O_4$ powders are spherical nanostructured particles composed of primary particles with a few tens of nanometer in size. The particle size distribution of $LiMn_2O_4$ powders synthesized at L_s = 100 mm and U_0/U_{mf} = 6.5 is shown in Figure 6. The geometric mean diameter $d_{g,p}$ and the geometric standard deviation σ_g of as-prepared particles were 0.81 μm and 1.85, respectively. This suggests that the $LiMn_2O_4$ powders can be synthesized with a narrow size dis-

Table 2. Chemical Composition, Geometric Mean Diameters, and Geometric Standard Deviation of As-Prepared Powders

U_0/U_{mf} [−]	Mn/Li [−]	$d_{p,g}$ [μm]	σ_g [−]
2.7	1.98	0.83	1.90
4.6	1.99	0.86	1.84
6.5	1.97	0.81	1.85
8.3	1.99	0.82	1.82

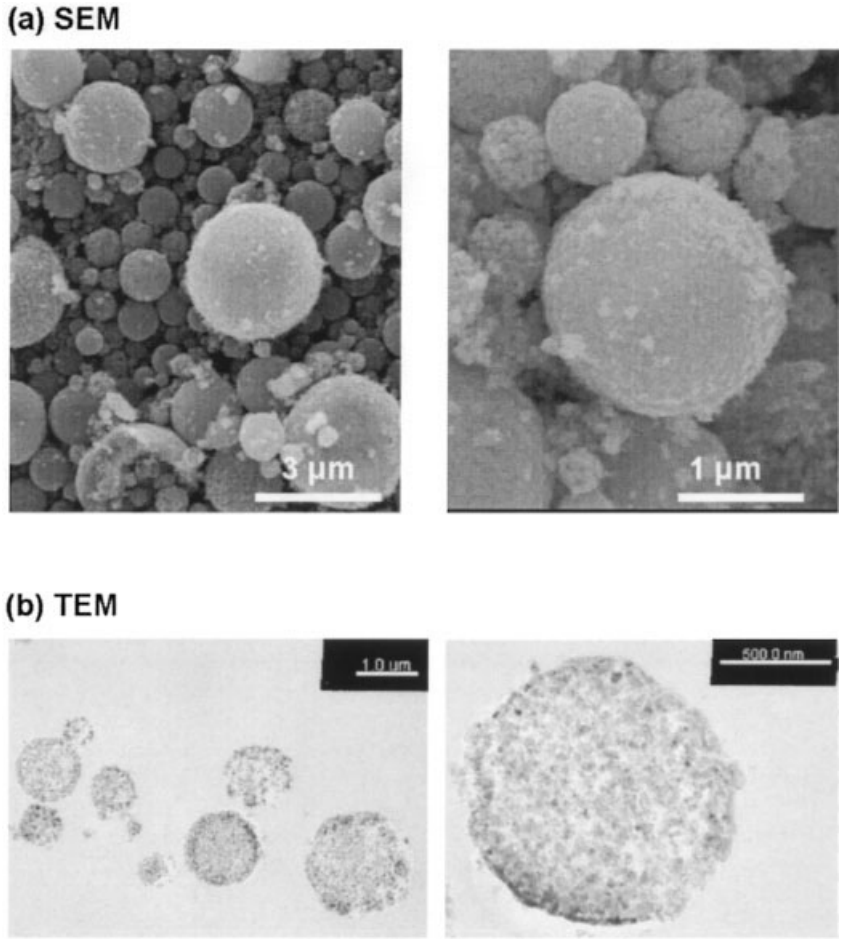

Figure 5. SEM and TEM photographs of $LiMn_2O_4$ synthesized at L_s = 100 mm, $d_{pm,g}$ = 498 μm, and U_0/U_{mf} = 6.5.

tribution using the spray pyrolysis and fluidized bed hybrid system. The geometric mean diameter and geometric standard deviation of the $LiMn_2O_4$ prepared at L_s = 100 mm for the range U_0/U_{mf} = 2.7-8.3 are also shown in Table 2. These results suggest that the spherical nanostructured powders with a narrow size distribution approximately 1 μm can be synthesized using the spray pyrolysis and fluidized bed hybrid system.

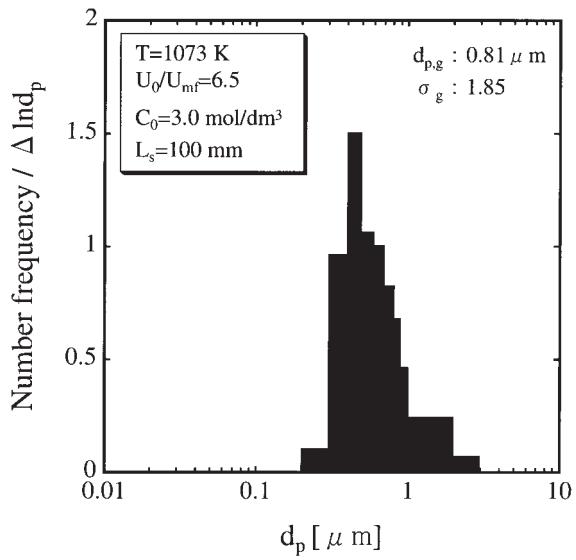

Figure 6. Particle size distribution of $LiMn_2O_4$ synthesized at L_s = 100 mm, $d_{pm,g}$ = 498 μm, and U_0/U_{mf} = 6.5.

Effects of process parameters on powder properties

Figure 7 shows the effects of fluidization number U_0/U_{mf} on crystallite size of as-prepared $LiMn_2O_4$ at L_s = 100 mm. The crystallite size of as-prepared $LiMn_2O_4$ gradually decreases with increasing fluidization number, and its size is larger than the one of the $LiMn_2O_4$ synthesized by conventional spray pyrolysis (L_s = 0 mm) in each fluidization number. However, the crystallite size becomes similar to the one of $LiMn_2O_4$ prepared at L_s = 0 mm with increasing fluidization number. The effect of fluidization number on the specific surface area of as-prepared $LiMn_2O_4$ is shown in Figure 8. In contrast with the case of crystallite size, the specific surface area of as-prepared $LiMn_2O_4$ gradually increases with the fluidization number, and its value is smaller than the one of the $LiMn_2O_4$ synthesized by conventional spray pyrolysis in each fluidization number. These results may explain why the residence time of $LiMn_2O_4$ particles in the reactor becomes longer with decreasing fluidization number and the sintering of $LiMn_2O_4$ progresses with decreasing fluidization number. As a result, the specific surface

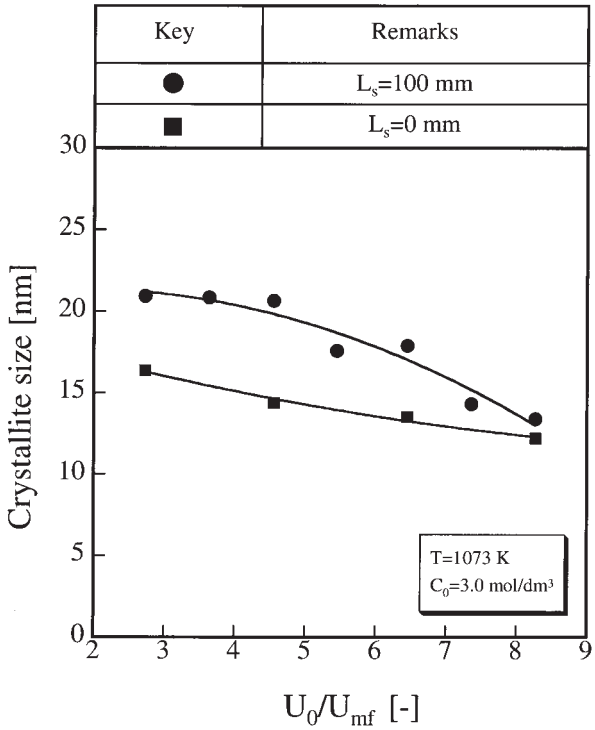

Figure 7. Effect of fluidization number U_0/U_{mf} on crystallite size of as-prepared $LiMn_2O_4$ at L_s = 100 mm and $d_{pm,g}$ = 498 μm.

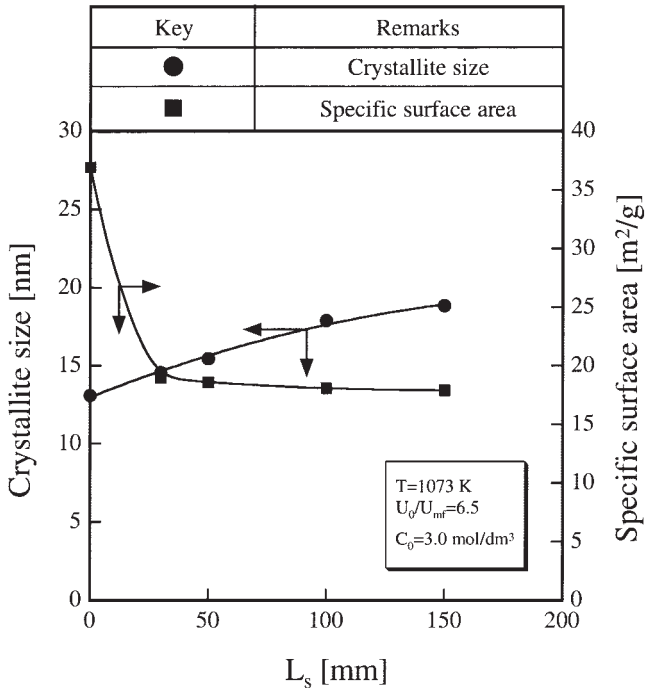

Figure 9. Effect of static bed height L_s on the crystallite size and specific surface area of $LiMn_2O_4$ powders synthesized by the spray pyrolysis and fluidized bed hybrid system at U_0/U_{mf} = 6.5 and $d_{pm,g}$ = 498 μm.

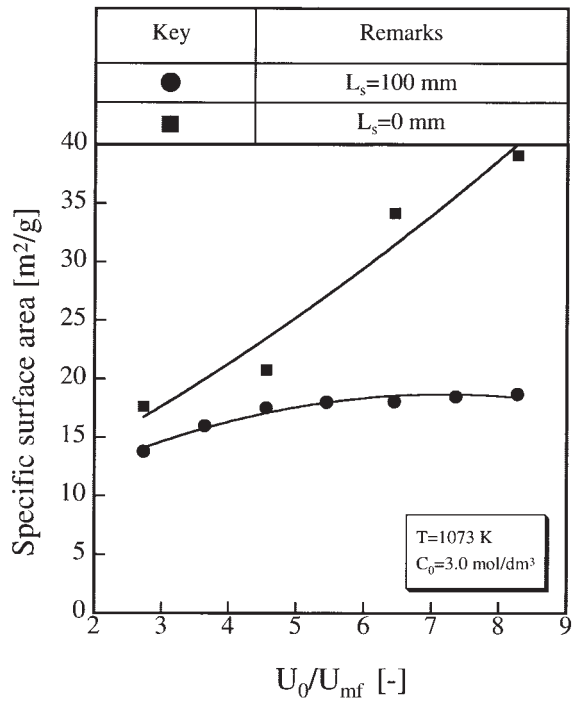

Figure 8. Effect of fluidization number U_0/U_{mf} on the specific surface area of as-prepared $LiMn_2O_4$ at $d_{pm,g}$ = 498 μm.

area decreases with decreasing fluidization number, and the crystallite size increases with decreasing fluidization number.

Figure 9 shows the effects of static bed height L_s on the crystallite size and specific surface area of $LiMn_2O_4$ powders synthesized using the spray pyrolysis and fluidized bed hybrid system at U_0/U_{mf} = 6.5. The specific surface area decreases with increasing static bed height, down to a fixed value of approximately 18 m^2/g, whereas the crystallite size increases from 13 nm up to 19 nm with static bed height. This may explain why the residence time of $LiMn_2O_4$ particles in the reactor becomes longer with static bed height and the sintering of $LiMn_2O_4$ progresses with increasing static bed height at a fixed fluidization number U_0/U_{mf}.

Figure 10 shows the variations of crystallite size and specific surface area of as-prepared $LiMn_2O_4$ powders with superficial gas velocity U_0 for the medium particle sizes of $d_{pm,g}$ = 294 μm and 498 μm. The specific surface area increases with superficial gas velocity, and the crystallite size decreases with increasing superficial gas velocity for the medium particle sizes of $d_{pm,g}$ = 294 μm and 498 μm. However, the larger the medium particles, the smaller the specific surface area and the larger the crystallite size at the same superficial gas velocity. This result may be due to the difference of fluidization behavior in the reactor between the medium particle sizes of $d_{pm,g}$ = 294 μm and 498 μm. Indeed, when all the data for the specific surface area and crystallite size of the as-prepared $LiMn_2O_4$ powders are plotted against the fluidization number U_0/U_{mf} (Figure 11), the specific surface area increases with superficial gas velocity, and the crystallite size decreases with increasing

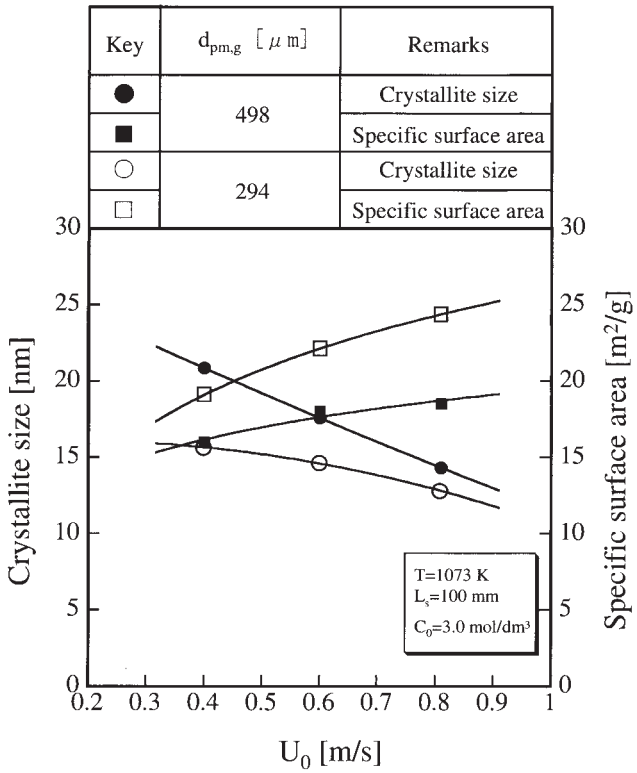

Figure 10. Variation of crystallite size and specific surface area of as-prepared $LiMn_2O_4$ powders with superficial gas velocity U_0 for medium particle size $d_{pm,g}$ = 294 μm and 498 μm.

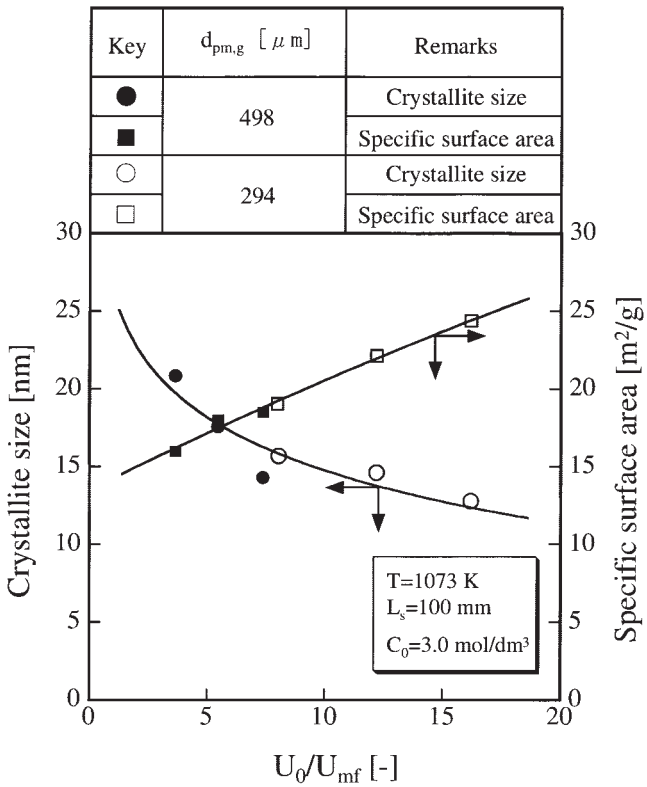

Figure 11. Variation of crystallite size and specific surface area of as-prepared $LiMn_2O_4$ powders with fluidization number U_0/U_{mf}.

superficial gas velocity on trend lines that are independent of medium particle size. These results show a good correlation between powder properties and the fluidization behavior.

In our previous works,[12,13] it was clearly observed that the smaller the specific surface area and the larger the crystallite size, the better the cycle performance, and the spherical dense particles were also suitable as cathode active materials for lithium-ion batteries. Thus, the $LiMn_2O_4$ materials prepared using the spray pyrolysis and fluidized bed hybrid system may be superior to those prepared by the conventional spray pyrolysis in battery performance. To confirm this prediction, we investigated the electrochemical properties of the studied samples using spring cells.

Electrochemical properties

The $LiMn_2O_4$ powders prepared at U_0/U_{mf} = 6.45, L_s = 150 mm, and C_0 = 3.00 mol/dm^3 were used as cathode active materials for lithium-ion batteries, and then the Li/1M $LiClO_4$ in PC/$LiMn_2O_4$ half cells was fabricated. The charge and discharge curves of the cell in the first cycle are shown in Figure 12. The cell was initially charged at a rate of 0.2 mA/cm^2 to the upper limit of 4.4 V. Upon discharge, the lower potential limit was 3.5 V. The charge and discharge curves showed two distinct plateaus, which indicates the well-defined spinel $LiMn_2O_4$ structure and is a characteristic of the manganese oxide spinel structure. The current charge and discharge capacities were 135 and 121 mAh/g in the first cycle, respectively, and its irreversible capacity was 12% in the first cycle.

Figure 13 shows the variations in discharge capacities with

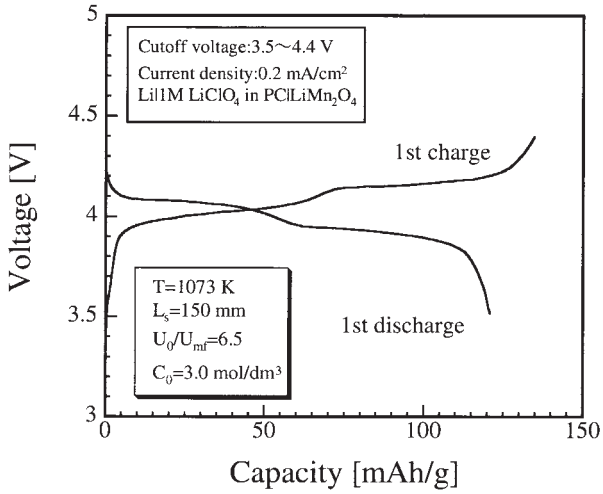

Figure 12. First charge and discharge curves of the electrochemical cell Li/1M $LiClO_4$ in PC/$LiMn_2O_4$ at current density of 0.2 mA/cm^2, where the cathode active materials were synthesized at U_0/U_{mf} = 6.45, L_s = 150 mm, $d_{pm,g}$ = 498 μm, and C_0 = 3.00 mol/dm^3 by the present method.

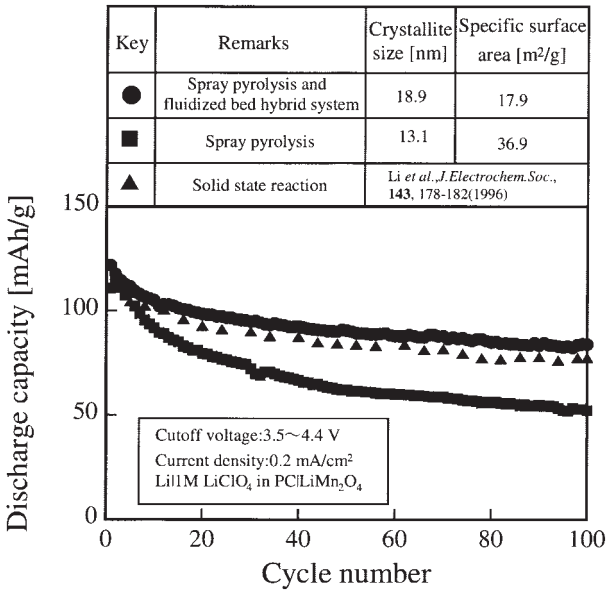

Figure 13. Variation of discharge capacities with the number of cycles for the Li/1M $LiClO_4$ in PC/$LiMn_2O_4$ cells at current density of 0.2 mA/cm^2, where the cathode active materials were synthesized at U_0/U_{mf} = 6.45, L_s = 150 mm, $d_{pm,g}$ = 498 μm, and C_0 = 3.00 mol/dm^3 by the present method.

the number of cycles for the Li/1M $LiClO_4$ in PC/$LiMn_2O_4$ cells, where the cathode active materials were synthesized at U_0/U_{mf} = 6.45, L_s = 150 mm, and C_0 = 3.00 mol/dm^3 by the present method. For comparison, the discharge capacity data for the samples synthesized by the solid-state reaction[26] and the conventional spray pyrolysis method (L_s = 0 mm) were also plotted in the figure. The present sample exhibited a larger discharge capacity and better cycling behavior than those prepared by the solid-state reaction and conventional spray pyrolysis method.

Conclusions

A spray pyrolysis and fluidized bed hybrid system has been developed for directly producing fine ceramic powders from a liquid solution. Using this system, the spinel $LiMn_2O_4$ powders were successfully prepared under various superficial gas velocities U_0 = 0.30-0.91 m/s, static bed heights L_s = 50-150 mm, and medium particle sizes $d_{pm,g}$ = 294-498 μm. The as-prepared samples exhibited a pure cubic spinel structure without any impurities in the XRD patterns, and the chemical composition of as-prepared powders showed good agreement with that of the precursor solution. The as-prepared $LiMn_2O_4$ powders have spherical nanostructured particles that consist of primary particles with a few tens of nanometer in size. The as-prepared powders showed larger crystallite size and smaller specific surface area than those prepared by conventional spray pyrolysis. Particle properties, such as crystallite size and specific surface area, were strongly affected by the residence (that is, sintering) time. Results show that both excess fluidization number and static bed height of the fluid bed medium are effective process control parameters.

To investigate the electrochemical characteristics of the as-prepared powders, Li/1M $LiClO_4$ in PC/$LiMn_2O_4$ cells were fabricated and their cycle performance was evaluated galvanostatically at room temperature. The as-prepared powders had larger discharge capacities and exhibited better cycling behavior than those prepared by the solid-state reaction and the conventional spray pyrolysis method.

Acknowledgments

This research was partially supported by the Ministry of Education, Culture, Sports Science and Technology of Japan (Grant No. 11650774). The authors are also grateful to the staff members (Mr. A. Genseki and Mr. J. Koki) of the Center for Advanced Materials Analysis (Tokyo Institute of Technology, Japan) for the analysis of as-prepared powders.

Literature Cited

1. Kato K, Onozawa I, Noguchi Y. Heat transfer in a dispersed bed. *J Chem Eng Japan.* 1983;16:178-182.
2. Kono HO, Huang CC, Morimoto E, Nakayama T, Hikosaka T. Segregation and agglomeration of Type C powders from homogeneously aerated type A-C powder mixtures during fluidization. *Powder Technol.* 1987;53:163-168.
3. Atwater JE, Akse JR, Wang TC, Kimura S, Johnson DC. Preparation of silicon-carbide-coated activated carbon using a high-temperature fluidized bed reactor. *Chem Eng Sci.* 2001;56:2685-2693.
4. Zhu Y, Li C, Wu Q. The process of coating on ultrafine particles by surface hydrolysis reaction in a fluidized bed reactor. *Surface Coating Technol.* 2000;135:14-17.
5. Hakim LF, Blackson J, George SM, Weimer AW. Nanocoating individual silica nanoparticles by atomic layer deposition in a fluidized bed reactor. *Chem Vap Deposition.* 2005;11:420-425.
6. Mu X, Bartmann U, Guraya M, Busser GW, Weckenmann U, Fischer R, Muhler M. The preparation of Pd/SiO_2 catalysts by chemical vapor deposition in a fluidized-bed reactor. *Appl Catal A.* 2003;248:85-95.
7. Lee JM, Kim YJ, Lee WJ, Kim SD. Coal-gasification kinetics derived from pyrolysis in a fluidized-bed reactor. *Energy.* 1998;23:475-488.
8. Ma X, Kaneko T, Guo Q, Xu G, Kato K. Removal of SO_2 from flue gas using a new semidry flue gas desulfurization process with a powder-particle spouted bed. *Can J Chem Eng.* 1999;77:356-362.
9. Chauk SS. Agnihotri R, Jadhave RA, Misro SK, Fan LS. Kinetics of high-pressure removal of hydrogen sulfide using calcium oxide powder. *AIChE J.* 2000;46:1157-1167.
10. Matsuda K, Furubayashi H, Taniguchi I. Synthesis of spinel $LiMn_2O_4$ powders by the drip pyrolysis in fluidized bed reactor. *J Chem Eng Japan.* 2005;38:316-321.
11. Huang H, Chen CH, Perego RC, Kelder EM, Chen L, Schoonman J, Weydanz WJ, Nielsen DW. Electrochemical characterization of commercial lithium manganese oxide powders. *Solid State Ionics.* 2000; 127:31-42.
12. Matsuda K, Taniguchi I. Relationship between the electrochemical and particle properties of $LiMn_2O_4$ prepared by ultrasonic spray pyrolysis. *J Power Sources.* 2004;132:156-160.
13. Matsuda K, Taniguchi I. Particle properties of $LiMn_2O_4$ fabricated by ultrasonic spray pyrolysis method. *Kagaku Kogaku Ronbunshu.* 2003; 29:232-237.
14. Taniguchi I, Lim CK, Song D, Wakihara M. Particle morphology and electrochemical performances of spinel $LiMn_2O_4$ powders synthesized using ultrasonic spray pyrolysis method. *Solid State Ionics*. 2002;146: 239-247.
15. Wu XM, Li XH, Xiao ZB, Liu J, Yan WB, Ma MY. Synthesis and characterization of $LiMn_2O_4$ powders by the combustion-assisted sol-gel technique. *Mater Chem Physics.* 2004;84:182-186.
16. Lu CH, Saha SK. Morphology and electrochemical properties of $LiMn_2O_4$ powders derived from the sol-gel route. *Mater Sci Eng.* 2001;B79:247-250.

17. Naghash AR, Lee JY. Preparation of spinel lithium manganese oxide by aqueous co-precipitation. *J Power Sources.* 2000;85:284-293.
18. Qiu X, Sun X, Shen W, Chen N. Spinel $Li_{1+x}Mn_2O_4$ synthesized by coprecipitation as cathodes for lithium-ion batteries. *Solid State Ionics.* 1997;93:335-339.
19. Du K, Zhang H. Preparation and performance of spinel $LiMn_2O_4$ by a citrate route with combustion. *J Alloy Comp.* 2003;352:250-254.
20. Yang W, Liu Q, Qiu W, Lu S, Yang L. A citric acid method to prepare $LiMn_2O_4$ for lithium-ion batteries. *Solid State Ionics.* 1999;121:79-84.
21. Choy JH, Kim DH, Kwon CW, Hwang SJ, Kim YI. Physical and electrochemical characterization of nanocrystalline $LiMn_2O_4$ prepared by a modified citrate route. *J Power Sources.* 1999;77:1-11.
22. Kanamura K, Dokko K, Kaizawa T. Synthesis of spinel $LiMn_2O_4$ by a hydrothermal process in supercritical water with heat-treatment. *J Electrochem Soc.* 2005;152:A391-A395.
23. Taniguchi I, Song D, Wakihara M. Electrochemical properties of $LiM_{1/6}Mn_{11/6}O_4$ (M =Mn, Co, Al and Ni) as cathode materials for Li-ion batteries prepared by ultrasonic spray pyrolysis method. *J Power Sources.* 2002;109:333-339.
24. Kato K, Takarada T, Matsuo N, Suto T, Nakagawa N. Residence time distribution of fine particles in a powder-particle fluidized bed. *Kagaku Kogaku Ronbushu.* 1991;17:970-975.
25. Wen CY, Yu YH. A generalized method for predicting the minimum fluidization velocity. *AIChE J.* 1966;12:610-612.
26. Li G, Ikuta H, Uchida T, Wakihara M. The spinel phases $LiM_yMn_{2-y}O_4$(M=Co,Cr,Ni) as the cathode for rechargeable lithium batteries. *J Electrochem Soc.* 1996;143:178-182.

Manuscript received Nov. 30, 2005, and revision received Feb. 24, 2006.